

Supplementary Material for

# Two-dimensional Phosphorus Carbide as Promising Anode Materials for Lithium-ion Batteries

Wei Zhang, Jiuren Yin, Ping Zhang\*, Xianqiong Tang, Yanhuai Ding\*

College of Civil Engineering & Mechanics, Xiangtan University, Hunan 411105, China

\*E-mail: [zhangp@xtu.edu.cn](mailto:zhangp@xtu.edu.cn); [yhding@xtu.edu.cn](mailto:yhding@xtu.edu.cn)

## 1. Kinetic and thermal stability calculation

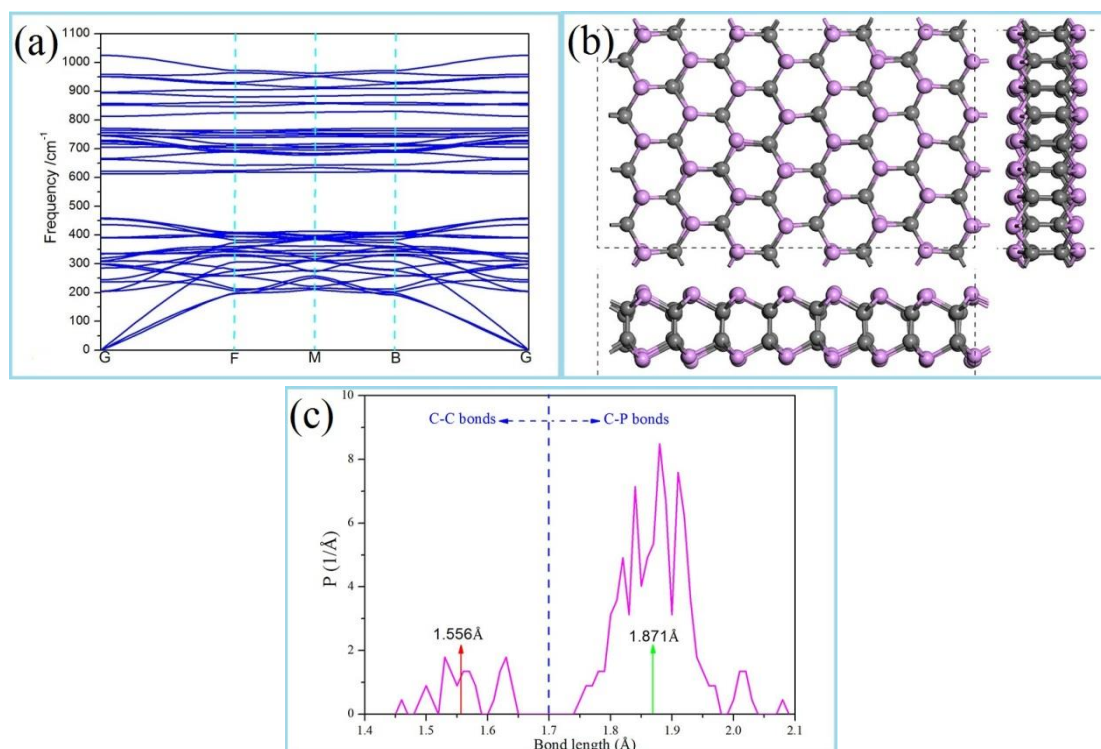


**Figure s1.** (a) The phonon dispersion curves of monolayer  $\gamma$ -PC. (b) Top and side

views of AIMD simulations for monolayer  $\gamma$ -PC at T=500K. **(c)** The distribution of bond length after AIMD simulation. The red and green arrows stand for the C-C and C-P bond length at T=0K, respectively.

## 2. Mechanical properties calculation

The calculations of mechanical properties of monolayer  $\gamma$ -PC are listed as follows. For 2D materials, the elastic constants and moduli can be calculated from Hooke's law under plane-stress condition,<sup>1,2</sup>

$$\begin{bmatrix} \sigma_{xx} \\ \sigma_{yy} \\ \sigma_{xy} \end{bmatrix} = \frac{1}{1-\nu_{xy}\nu_{yx}} \begin{bmatrix} E_x & \nu_{yx}E_x & 0 \\ \nu_{xy}E_y & E_y & 0 \\ 0 & 0 & G_{xy}(1-\nu_{xy}\nu_{yx}) \end{bmatrix} \begin{bmatrix} \varepsilon_{xx} \\ \varepsilon_{yy} \\ 2\varepsilon_{xy} \end{bmatrix} = \begin{bmatrix} C_{11} & C_{12} & 0 \\ C_{21} & C_{22} & 0 \\ 0 & 0 & C_{66} \end{bmatrix} \begin{bmatrix} \varepsilon_{xx} \\ \varepsilon_{yy} \\ 2\varepsilon_{xy} \end{bmatrix} \quad (1)$$

$$E_x = \frac{C_{11}C_{22} - C_{12}C_{21}}{C_{22}}, \quad E_y = \frac{C_{11}C_{22} - C_{12}C_{21}}{C_{11}}, \quad \nu_{xy} = \frac{C_{21}}{C_{22}}, \quad \nu_{yx} = \frac{C_{12}}{C_{11}}, \quad G_{xy} = C_{66} \quad (2)$$

where  $E_i = \frac{\sigma_i}{\varepsilon_i}$  ( $i = x, y$ ) represents the Young's modulus along the axis of  $i$ ,

$\nu_{ij} = -\frac{d\varepsilon_j}{d\varepsilon_i}$  is the Poisson's ratio with tensile strain applied in the direction  $i$  and

the response strain in the direction  $j$ .

The relationship between the strain energy and the applied strains can be expressed as formula (3):

$$E_s = a_1\varepsilon_{xx}^2 + a_2\varepsilon_{yy}^2 + a_3\varepsilon_{xx}\varepsilon_{yy} + a_4\varepsilon_{xy}^2 \quad (3)$$

Where  $E_s = E(\varepsilon) - E_0$  is the strain energy calculated from the energy difference between strained and no strained structures.

The elastic stiffness constants can be calculated with equation (4):

$$C_{ij} = \frac{1}{A_0 d_0} \left( \frac{\partial E_s^2}{\partial \varepsilon_i \partial \varepsilon_j} \right) \quad (4)$$

where  $i, j = xx, yy, xy$ ,  $A_0$  is the area of the structure in  $xy$  plane and  $d_0$  is the effective thickness of the structure.

From formula (3) and (4), we derive the Young's moduli, shear moduli and Poisson's ratios for the structures as a function of  $a_i$  as formula (5):

$$E_x = \frac{4a_1 a_2 - a_3^2}{2a_2 A_0 d_0}, E_y = \frac{4a_1 a_2 - a_3^2}{2a_1 A_0 d_0}, G_{xy} = \frac{2a_4}{A_0 d_0}, \nu_{xy} = \frac{a_3}{2a_2}, \nu_{yx} = \frac{a_3}{2a_1} \quad (5)$$

The Young's modulus along an arbitrary direction can be calculated from the formula (6)<sup>2</sup>:

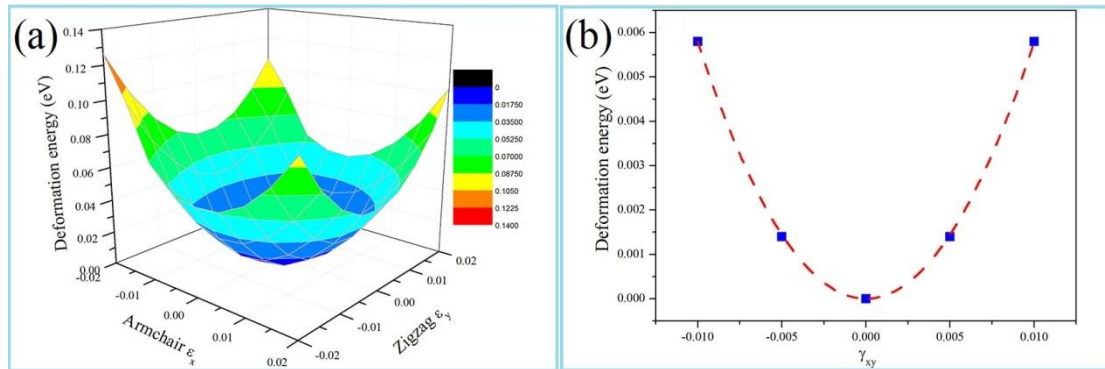
$$\frac{1}{E_\varphi} = S_{11} \cos^4 \varphi + (2S_{12} + S_{66}) \cos^2 \varphi \sin^2 \varphi + S_{22} \sin^4 \varphi \quad (6)$$

where  $\varphi \in [0, 2\pi]$ , is the angle of an arbitrary direction from  $+x$  axis,  $E_\varphi$  is the Young's modulus along  $\varphi$  direction,  $S_{ij}$  represents elastic compliance constants, which can be calculated from formula (7):

$$S_{11} = \frac{C_{22}}{C_{11}C_{22} - C_{12}^2}, S_{22} = \frac{C_{11}}{C_{11}C_{22} - C_{12}^2}, S_{12} = \frac{-C_{12}}{C_{11}C_{22} - C_{12}^2}, S_{66} = \frac{1}{C_{66}} \quad (7)$$

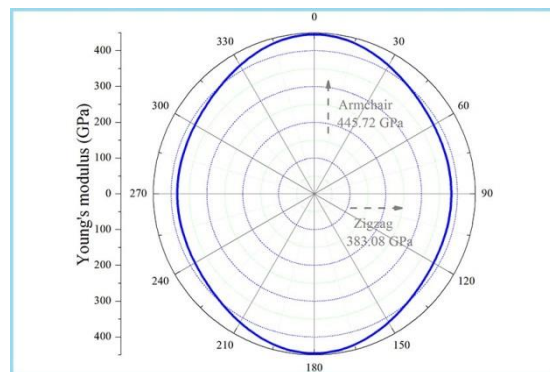
(i) We calculated the Young's modulus, shear modulus and Poisson's ratios firstly. The strain along armchair or zigzag direction ranged from -0.02 to 0.02 with an increasing step of 0.005. Then, the corresponding energy changes were collected and plotted in figure s3 (a). Through quadric surface fitting the strain-energy curved surface, the

coefficients  $a_1$ ,  $a_2$ ,  $a_3$  in formula (3) can be determined.  $a_4$  can be calculated by parabolic fitting the energy & shear strains points plotted in figure s3 (b). From formula (5), the Young's modulus, shear modulus and Poisson's ratios can be determined.

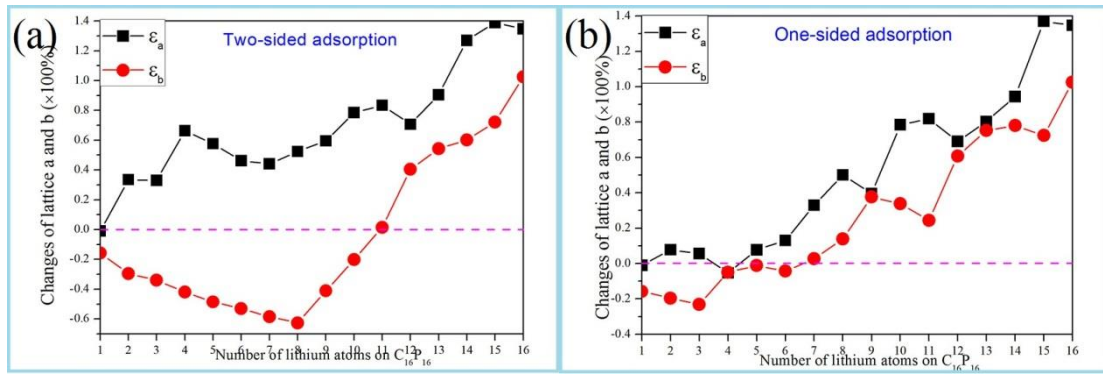


**Figure s2.** (a) The three-dimensional energy curved surface with corresponding strains. (b) The energy difference between the relaxed and shear strained monolayer  $\gamma$ -PC.

(ii) Through formula (3), (4) and (7), we can get the elastic compliance constants  $S_{ij}$  and then put them into the formula (6) to gain the relationship between Young's modulus and directions.

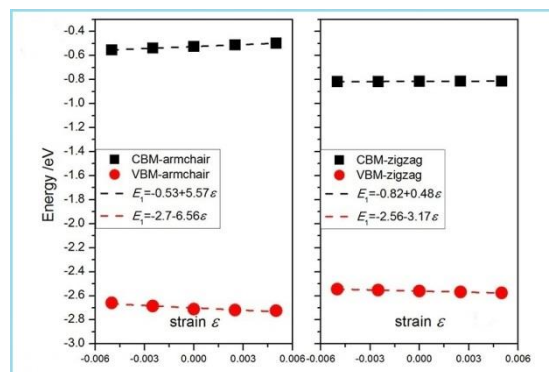


**Figure s3.** The direction dependence of Young's modulus for monolayer  $\gamma$ -PC.



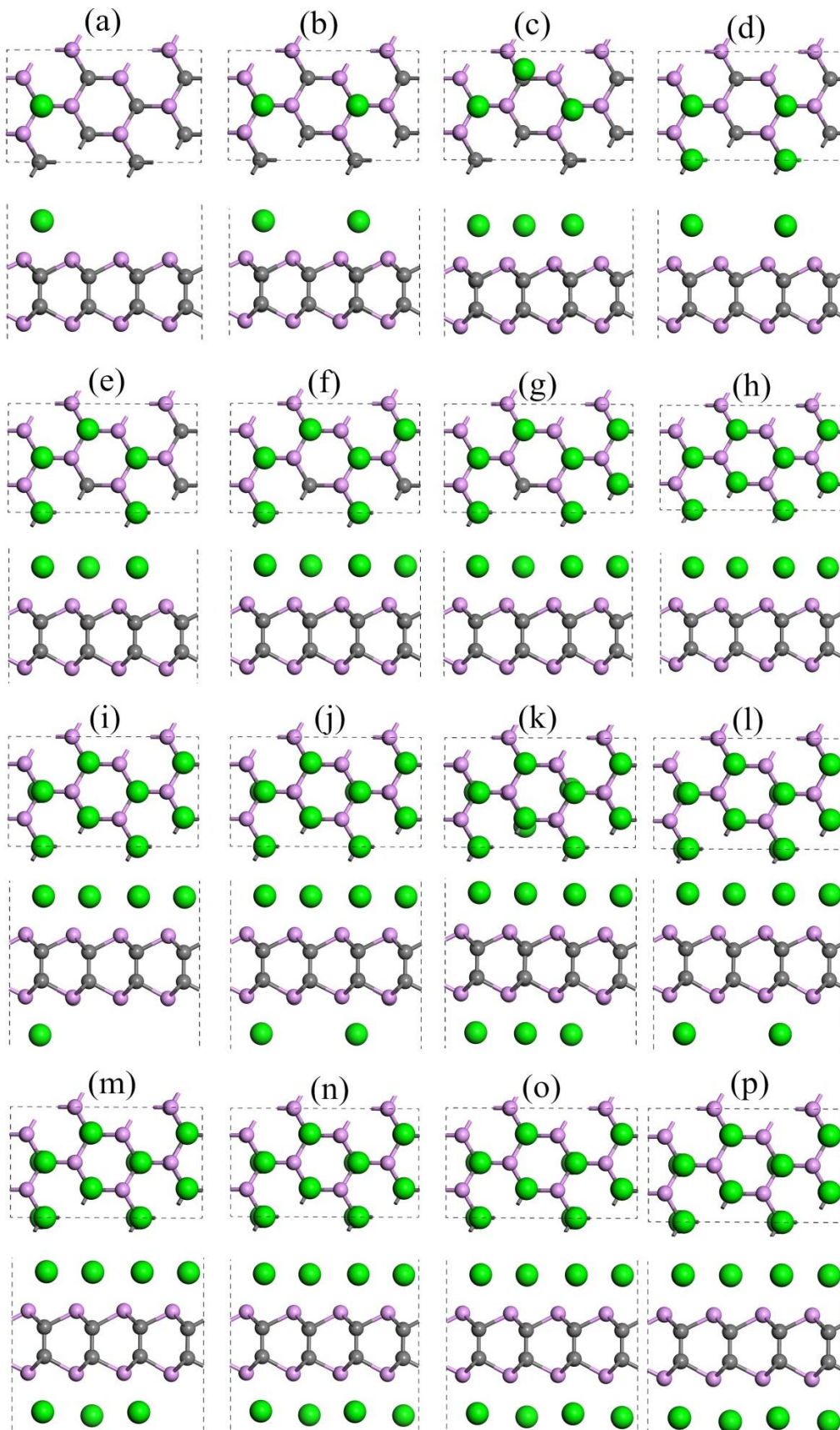
**Figure s4.** The lattice changes of the lithiation  $P_{16}C_{16}$  for **(a)** two-sided adsorption and **(b)** one-sided adsorption with corresponding numbers of adsorbed Li atoms.

### 3. Conductivity calculation



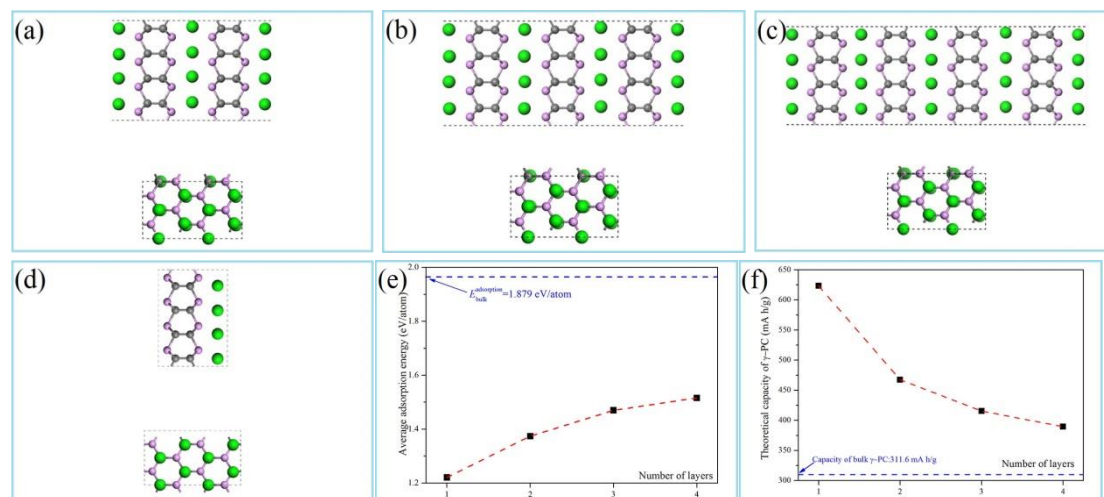
**Figure s5.** Energy shift of CBM and VBM for monolayer  $\gamma$ -PC with respect to the lattice dilation and compression along the zigzag and armchair directions, respectively.

### 4. Capacity calculation



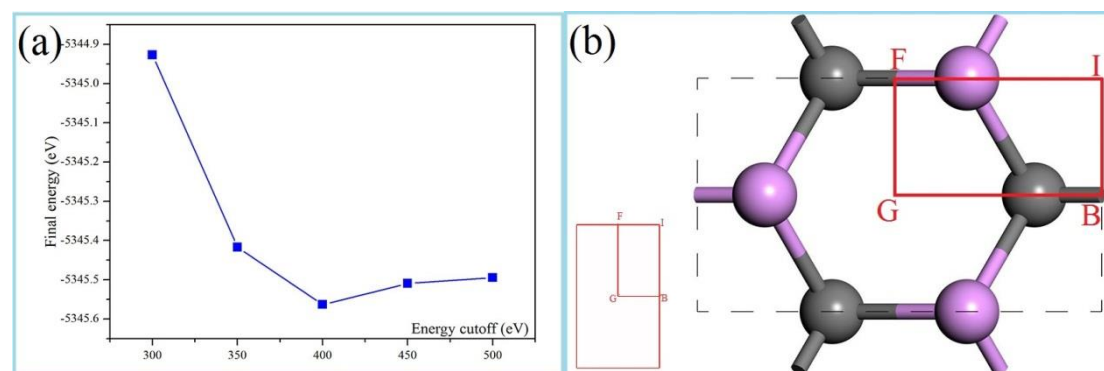
**Figure s6.** Top and side views of the most stable structures at different x values of

$P_{16}C_{16}Li_x$ , the x values are 1, 2, 3...16 for **(a)**, **(b)**, **(c)**...**(p)**, respectively. Noted that, the Li adsorption starts from one-sided filling (a~h) to two-sided storing (i~p).



**Figure s7.** Side and top views of fully adsorbing for Li onto **(a)** two-layers, **(b)** three layers, **(c)** four layers and **(d)** bulk  $\gamma$ -PC in AA stacking with corresponding **(e)** average adsorption energy and **(f)** capacity.

## 5. Setting of calculation



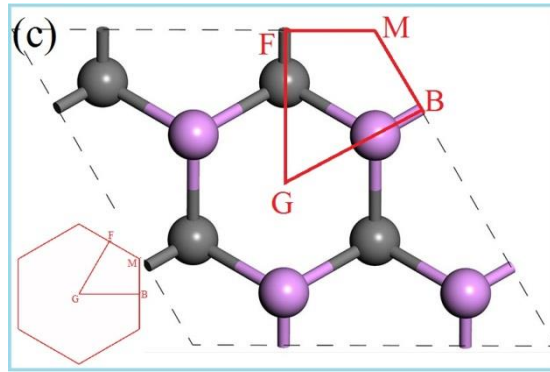


**Figure s8. (a)** The total energy of  $P_{16}C_{16}$  at different cutoff energy when Monkhorst-Pack K-point mesh is set as  $3 \times 4 \times 1$ . The integration path in Brillouin zone used for **(b)** electronic structure calculations and **(c)** phonon dispersion calculations.

### **References**

1. Zhou, J.; Huang, R., Internal lattice relaxation of single-layer graphene under in-plane deformation. *J. Mech. Phys. Solids* 2008, 56, 1609-1623.
2. Wei, Q.; Peng, X., Superior mechanical flexibility of phosphorene and few-layer black phosphorus. *Appl. Phys. Lett.* 2014, 104, 372-98.